Inhibitor discovery of phospholipases and N-acyltransferases

Zhou, J.

3

Structure activity relationship of α-ketoamides on phospholipase-acyltransferases: discovery of LEI110

3.1 Introduction

The human phospholipase A/acyl transferase (PLAAT) family consists of five members (namely, PLAAT1-5) of which two are absent in rodents (i.e. PLAAT2, and PLAAT4).[1, 2] PLAAT enzymes show structural homology to lecithin retinol acyl transferase (LRAT) and belong to the NIpC/P60 superfamily of cysteine proteases.[3] The members of the PLAAT family share a highly conserved NCEHFV peptidic sequence, which includes the catalytically active cysteine residue.[4] The catalytic cysteine forms a catalytic triad with two N-terminal histidines in PLAAT2-5 and an N-terminal histidine together with an asparagine in PLAAT1. PLAATs possess Ca^{2+}-independent phospholipase activity *in vitro* with both phosphatidylcholine (PC) and phosphatidylethanolamine (PE) acting as substrates. All members also exhibit *O*-acyl transferase activity with preference for the *sn*-1 position of lysophosphatidylcholine (lysoPC) as well as *N*-acyltransferase activity with the ability to produce *N*-acylphosphatidylethanolamines (NAPEs) through catalysis of the acyl chain transfer from the *sn*-1 position of glycerophospholipids to the amine function of PE.[2] All enzymes, except PLAAT3, show a preference for PLA_1 activity (hydrolysis of phospholipids to produce 2-acyl-lysophospholipids and fatty acids) over PLA_2 activity (hydrolysis of the sn-2 position of membrane glycerophospholipids to liberate arachidonic acid). Depending on the assay conditions the substrate preference of PLAAT3 may shift. For example, Duncan *et al.* reported that PLAAT3 has a preference for the *sn-2* position with a moderate Ca^{2+}-dependency,[5] while Uyama *et al.* found primarily hydrolysis of the fatty acyl at the *sn-1* position.[6]

The structures of PLAAT2 and PLAAT3 have been solved through X-ray crystallography.[7] Both proteins contain three alpha helices separated from a four stranded anti-parallel beta sheet. The proteins also contain a C-terminal transmembrane hydrophobic domain, with the exception of PLAAT5, which was proposed to anchor the protein in the lipid membrane. The C-terminal domain of these proteins has been shown to be required for subcellular localization, as the truncated form of the PLAAT3-GFP fusion protein has been found to be evenly diffused in COS-7 cells. The full length fusion protein on the other hand showed a predominantly perinuclear localization and to a lesser extent localization in the cytoplasm.[5] In contrast, in HEK293 and HeLa cells PLAAT3 localization has been shown to be associated with peroxisomes.[8] Furthermore, deletion of the hydrophobic transmembrane C-terminal domain of PLAAT3 resulted in a total loss of phospholipase activity.[5]

PLAAT1 is predominantly expressed in human testes, skeletal muscle, and heart. Overexpression of PLAAT1 was shown to inhibit the growth of H-Ras-transformed NIH3T3 fibroblasts.[9] Furthermore, hypermethylation of CpG islands in the 5' region of the PLAAT1 gene, causing reduced expression of the protein, has also been shown in multiple gastric cancers.[10] A relatively high *N*-acyltransferase activity has been observed *in vitro*, compared to PLAAT2-5.[11] The

physiological role of the enzyme however has yet to be studied. PLAAT2 is expressed primarily in the human colon, small intestine, stomach, trachea and kidneys.[12] Overexpression of this protein resulted in reduced colony formation in HCT166 colon cancer cells, HeLa cervical cancer cells, and MCF-7 breast cancer cells. Moreover, overexpression of PLAAT2 in HtTA cervical cancer cells resulted in suppression of RAS activation and increased cell death. This effect was found to be dependent on the C-terminal hydrophobic domain. The enzyme was determined to have primarily *N*-acyltransferase activity *in vitro* and preferred the *sn-1* position of PC as acyl donor.[13] The physiological role of PLAAT2 has not been characterized, which is partly due to a lack of inhibitors.

PLAAT3 is the most studied member of the PLAAT proteins. The *in vivo* relevance of PLAAT3 has not been well studied, but a mouse model constitutively lacking the *hrasls3* gene has been generated.[14] Ablation of PLAAT3 prevented obesity caused by high fat diet feeding or leptin deficiency, thus establishing PLAAT3 as a potential target for the treatment of obesity. PLAAT3 deficient mice exhibited a higher rate of lipolysis, due to decreased levels of prostaglandin E_2 (PGE_2) that were most likely caused by a decrease in arachidonic acid levels. In addition, increased fatty acid oxidation in adipose tissue was also reported. Currently, there are no pharmacological tools to study the effects of acute and dynamic inhibition of PLAAT3.

The expression of PLAAT4 was decreased in a variety of primary human tumors, and cancer cell lines.[15] Similarly to other PLAAT members, this enzyme inhibited H-RAS mediated signaling. PLAAT4 primarily functions as a phospholipase *in vitro* and the activity has been observed to be dependent on the C-terminal domain.[2, 16] It is expressed in high levels in differentiated human keratinocytes where it regulates cell survival through interaction with type 1 transglutaminase (TG1), the enzyme responsible for the cornified envelope formation. In addition, reduced expression of PLAAT4 can be observed in psoriasis.[17] Currently, there are no chemical tools to study the effects of acute and dynamic inhibition of PLAAT4.

PLAAT5 primarily shows *N*-acyltransferase activity over *O*-acyltransferase and PLA1/2 *in vitro*.[2] It has been observed in rat spermatocytes although its function remains unknown.[18] As mentioned earlier, the enzyme is structurally different from the other PLAAT proteins as it does not contain the C-terminal transmembrane domain and therefore is predominantly found in the cytosol.[19] The physiological function of the enzyme remains unknown. Furthermore, it is also unknown if PLAAT5 acts as a tumor suppressor similar to the other PLAAT members. Ueda and coworkers overexpressed PLAAT5 in COS-7 cells and found that this protein could catalyze the formation of radioactive NAPE via transferring the radioactive acyl group from PC to PE. The activity of PLAAT5 was mainly found in cytosolic fraction and not stimulated by Ca^{2+}-ions.[19]

In chapter 3, an activity based protein profiling (ABPP) method was developed to measure PLAAT activity. Screening of a focused library resulted in the discovery of α-ketoamide **1** as a selective PLAAT inhibitor. In this chapter, a set of 63 analogues of compound **1** was tested for

their potency against PLAAT3, PLAAT4 and PLAAT5 using competitive ABPP, which led to the discovery of LEI110 as a potent and selective inhibitor for PLAAT3.

3.2 Results and discussion

To obtain a structure-activity relationship of α-ketoamides on PLAAT activity, an ABPP method was employed as developed in **Chapter 3**. In short, cytosol fractions of human embryonal kidney 293T cells (HEK293T) transiently overexpressing recombinant human PLAAT3, PLAAT4 or PLAAT5 were incubated with test compounds at 10 µM for 30 min and then with probe MB064 for another 20 min. The proteins were then resolved by sodium dodecyl sulfate polyacrylamide gel electrophoresis (SDS PAGE) and the residual protein activity was visualized by in-gel fluorescence scanning. First, a small set of structural analogues (**2**-**30**) of compound **1** were tested at a single concentration of 10 µM. The following structure-activity relationship could be derived (see Table 1). Compared to compound **1,** reducing the linker length either at the amine part (**2**) or α-keto part (**6**) reduced inhibitory activity. Of note, compound **2** showed selectivity for PLAAT3 over PLAAT4/5. Conversely, increasing the spacer length at the amine part increased the inhibitory activity (**3**). The inhibitory activity was abolished when the amide was methylated (**4, 9**) or ethylated (**5**). Substitution of 2-phenethylamine with various primary amines (**7**,**8**,**10**) retained activity, but secondary amines (**9**, **11**-**18**) did not yield promising inhibitors. β-Ketoamides (**19**, **20**) and α-(di)fluoro-substituted β-ketoamides (**21**-**24**) or reduced analogues (**26**-**28**) were not active. Importantly, reduction of the α-keto to the hydroxyl group in compound **25** led to a decrease in activity, suggesting that the α-keto forms an important interaction with the enzymes. Replacement of the α-keto warhead by an epoxide as an alternative electrophile did not yield an active inhibitor (**29**). Finally, compound **30** showed weak inhibitory activity. From these results, it is concluded that the α-keto and a secondary amide are essential for PLAAT inhibition.

Table 1. The pIC_{50} values of compounds **1-30** with standard deviations.

ID	Structure	PLAAT3	4	5	ID	Structure	PLAAT3	4	5
1	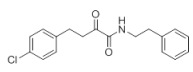	6.0±0.2	6.2±0.1	6.4±0.1	**16**	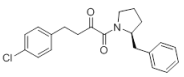	**<5**	**<5**	**<5**
2	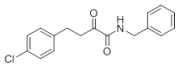	**5.8**±0.1	**<5**	**<5**	**17**	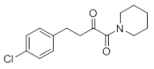	**<5**	**<5**	**<5**
3	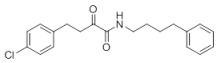	**6**±0.1	**5.8**±0.1	**6.7**±0.1	**18**	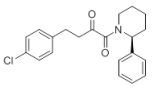	**<5**	**<5**	**<5**
4	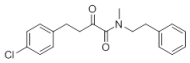	**<5**	**<5**	**<5**	**19**	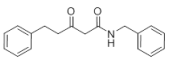	**<5**	**<5**	**<5**
5	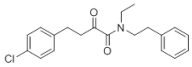	**<5**	**<5**	**<5**	**20**	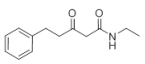	**<5**	**<5**	**<5**
6	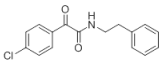	**<5**	**<5**	**<5**	**21**	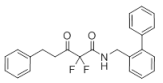	**<5**	**<5**	**<5**
7	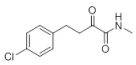	**5.2**±0.1	**5.4**±0.1	**6.1**±0.1	**22**	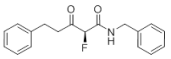	**<5**	**<5**	**<5**
8	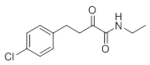	**5.1**±0.1	**5.4**±0.1	**6**±0.1	**23**	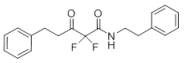	**<5**	**<5**	**<5**
9	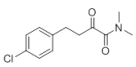	**<5**	**<5**	**<5**	**24**	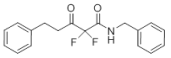	**<5**	**<5**	**<5**
10	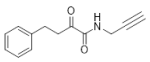	**<5**	**<5**	**5.6**±0.1	**25**	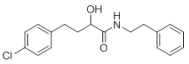	**<5**	**<5**	**<5**
11	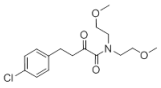	**<5**	**<5**	**<5**	**26**	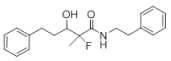	**<5**	**<5**	**<5**
12	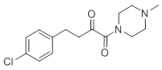	**<5**	**<5**	**<5**	**27**	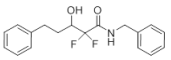	**<5**	**<5**	**<5**
13	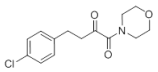	**<5**	**<5**	**<5**	**28**	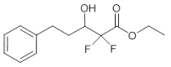	**<5**	**<5**	**<5**
14	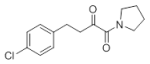	**<5**	**<5**	**<5**	**29**	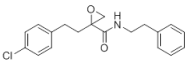	**<5**	**<5**	**<5**
15	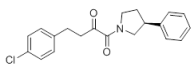	**<5**	**<5**	**<5**	**30**	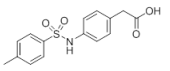	**<5**	**<5**	**<5**

In the next compound set, the phenethylamine was kept constant and different groups were incorporated at the other side of the molecule (Table 2). The inhibitors were tested

at five different concentrations (0.01, 0.1, 1, 10, and 100 μM) against PLAAT 3-5 and the dose-response curve was plotted to determine the pIC_{50}. Changing the location of the chlorine substituent to the *ortho*- (**31**) or *meta*-position (**32**) did not increase the potency compared to compound **1**. Incorporation of a 3,4-dichloro-substituent (**33**) slightly increased the inhibitory activities against these three enzymes. None of the other substituents (F, Me, OMe, CF_3) at the *para*-position (**34**-**38**) gave better inhibitors. However, removal of the chlorine (compound **39**) or elimination of the 4-Cl-phenyl moiety (compound **42**) led to an inactive compound at PLAAT3, but not at PLAAT5. Different linker lengths between the phenyl and the α-ketone (**40**, **41**, **43**) were explored. Notably, compound **40** with a three-carbon linker showed increased potency for PLAAT3 and 5.

Table 2. The pIC_{50} values of compound **1**, **31**-**43** with standard deviations.

ID	Structure	PLAAT3	4	5	ID	Structure	PLAAT3	4	5
1	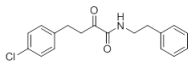	6.0±0.2	6.2±0.1	6.4±0.1	**37**	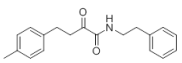	5.7±0.1	5.8±0.1	5.6±0.1
31	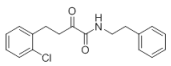	5.7±0.1	5.6±0.1	5.8±0.1	**38**	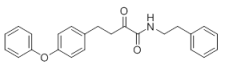	5.4±0.1	5.9±0.1	6.9±0.1
32	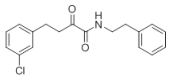	5.8±0.1	5.9±0.1	5.9±0.1	**39**	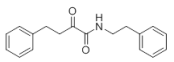	<5	5.5±0.1	6.0±0.1
33	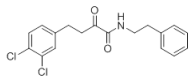	7.0 ± 0.2	6.0± 0.1	7.0±0.1	**40**	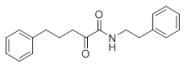	6.4±0.1	6.2±0.1	7.0±0.1
34	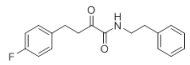	5.3±0.1	5.0±0.1	5.8±0.1	**41**	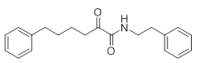	6.0±0.1	5.8±0.1	6.8±0.1
35	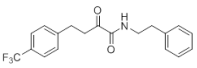	5.1±0.1	5.6±0.1	6.5±0.1	**42**	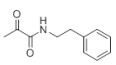	<5	<5	<5
36	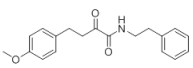	5.5± 0.1	5.9±0.1	5.9±0.1	**43**	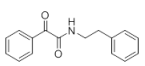	<5	<5	<5

Next, a series of β,γ-unsaturated α-ketoamides (**44**-**50**, Table 3) were tested to explore the effect of restricting the conformation of the alkyl linker. None of these compounds showed improved potency against PLAAT3-5. The structure-activity relationship (Table 2 and 3) indicates that the 3-phenylpropyl moiety (shown in compound **40**) is the optimal fragment for the α-keto side.

Table 3. The pIC_{50} values of compound **1**, **44**-**50** with standard deviations.

ID	Structure	PLAAT3	4	5	ID	Structure	PLAAT3	4	5
1	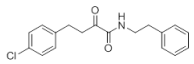	6.0±0.2	6.2±0.1	6.4±0.1	**47**	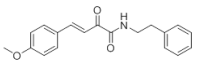	5.3±0.1	5.6± 0.07	6.0±0.1
44	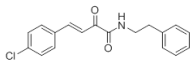	5.6±0.1	5.6±0.1	6.2±0.1	**48**	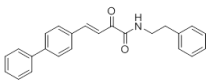	5.2±0.1	5.0± 0.1	5.6±0.1
45	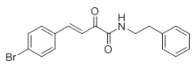	5.6±0.1	5.2±0.1	6.2± 0.1	**49**	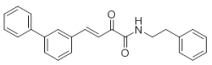	5.5±0.1	5.6± 0.1	6.0±0.1
46	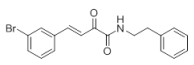	<5	5.1± 0.1	5.5± 0.1	**50**	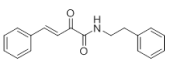	5.8±0.1	5.0± 0.1	5.2±0.2

Finally, with the optimal fragment (3-phenylpropyl) for the α-keto side in hand, it was decided to optimize the phenethylamine moiety (Table 4). Incorporation of small substituents on the *para*-position (**51**-**54**) resulted in different bioactivities. 4-Methyl-substituted compound (**51**) and 4-bromo analog (**53**) showed substantially increased inhibitory potency for PLAAT3 and PLAAT5 (pIC_{50}: 7.0±0.1 and 7.4±0.1, respectively), whereas more polar substituents, such as *p*-hydroxyl (**52),** 4-methoxy (**54**), 3,4-dimethoxy (**55**) did not increase the potency. Of note, para-substitution increased also the selectivity for PLAAT5. The 2-chloro analogue (**56**) showed decreased potency, while the 3-chloro (**57**) and 2,4-dichloro (**58**) derivatives showed increased potency for PLAAT3,5 and slightly decreased potency for PLAAT4. Finally, various aromatic rings (**59**-**64**) were incorporated at the *para*-position of the phenethylamine via an ether linkage. Compound **59** (phenyl-), **62** (6-(trifluoromethyl)pyridin-3-yl), **63** (5-(trifluoromethyl)pyridin-2-yl) and **64** (2-chloropyrimidin-4-yl) all showed increased inhibitory activities against PLAAT3-5.

Table 4. The pIC_{50} values of compound **1**, **51**-**64** with standard deviations.

ID	Structure	PLAAT3	4	5	ID	Structure	PLAAT3	4	5
1	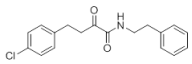	6.0±0.2	6.2±0.1	6.4±0.1	**58**	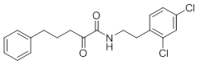	6.6±0.1	6.1±0.1	7.2±0.1
51	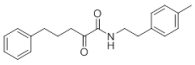	7.0±0.1	5.9±0.1	7.4±0.1	**59**	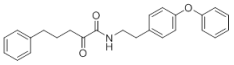	7.2±0.1	7.3±0.1	7.4±0.2
52	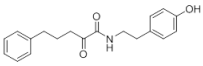	5.8±0.1	5.6±0.1	6.8±0.10	**60**	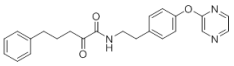	6.6±0.1	6.2±0.1	7.2±0.1
53	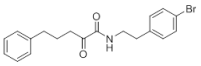	6.8±0.1	6.7±0.1	8.0±0.1	**61**	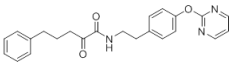	5.7±0.1	5.9±0.1	6.6±0.1
54	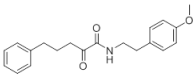	6.1±0.1	5.8±0.1	7.1±0.1	**62**	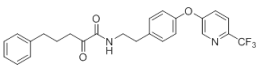	6.8±0.1	7.1±0.1	7.1±0.1
55	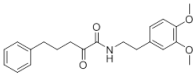	6.0±0.2	5.2±0.1	6.5±0.1	**63 (LEI110)**	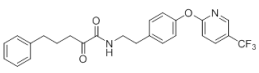	7.0±0.1	6.8±0.1	7.6±0.1
56	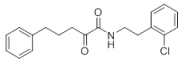	5.9±0.1	5.6±0.1	6.1±0.2	**64**	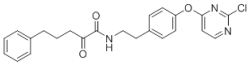	6.6±0.1	6.7±0.1	7.1±0.1
57	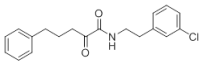	6.7±0.1	6.0±0.1	7.3±0.1					

In order to gain insight in the molecular interactions of α-ketoamides with PLAAT3, LEI110 (**63**) and **1** were docked in a PLAAT3 crystal structure (PDB: 4DOT).[7] It was envisioned that the electrophilic ketone of LEI110 and **1** could act through a reversible covalent mechanism with the active site Cys113 forming a hemithioacetal adduct (Figure 1B), similar to other reported α-ketoamide inhibitors.[20] This adduct was generated in silico for LEI110 and **1** after which molecular dynamics simulation was performed (Figure 1A). Hydrogen bonding of the oxyanion with His23 was observed in both cases, as well as π-π stacking with Tyr21. The extension of the ketone alkyl chain by one methylene allows for a more optimal π-cation interaction with Arg18 for LEI110, compared to **1**. Furthermore, the introduction of the pyridyl moiety in LEI110 enables an additional hydrogen bond with the Tyr21-OH. These docking results provide a potential explanation for the 10-fold increase in activity seen for LEI110.

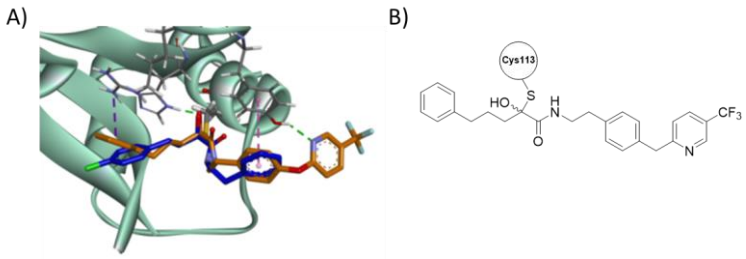

Figure 1. (A) Structure-guided modeling of **1** and LEI110. Compounds **1** (blue) and LEI110 (orange) in complex with PLAAT3, covalently bound to Cys113. Green dotted lines represent a hydrogen bond, pink and purple represent π-interactions. (B)the structure of the hemithioacetal adduct of LEI110.

3.3 Conclusions

In this chapter, an ABPP assay method was used to profile the inhibitory activities of the pan-PLAAT inhibitor **1** and 63 designed analogs and a structure-activity relationship was also developed. Based on the screening results of library 1 (Table 1), it was found that the α-keto and the secondary amide were essential for inhibition. Screening the focused compound libraries 2 (Table 2) and 3 (Table 3) with variation of the α-keto side of the molecule, the 3-phenylpropyl moiety (shown in compound **40**) is found to be the optimal fragment from the α-keto side. Further efforts were focused on the optimization of the phenethylamine moiety while having the 3-phenylpropyl moiety at the α-keto side. In the end, compound **52** and **53** were identified as potent and selective inhibitors for PLAAT5. Compound **51** and **63** (LEI110) were identified as potent and selective inhibitors for PLAAT3 and 5. Molecular dynamics simulations of LEI110 in the reported crystal structure of PLAAT3 provided insight in the potential ligand-protein interactions to explain its binding mode. LEI110 is the most potent and selective PLAAT3 inhibitor reported to date and provides a good starting point for further structure-based inhibitor development for PLAAT3.

4.4 Experimental procedures

Plasmids. Full-length human cDNA of PLAAT3 (kindly provided by Prof. N. Ueda, Department of Biochemistry, School of Medicine, Kagawa University, 1750-1 Ikenobe, Miki, Kagawa 761-0793, Japan) was cloned into mammalian expression vector pcDNA3.1, containing genes for ampicillin and neomycin resistance. The inserts were cloned in frame with a C-terminal FLAG-tag and site-directed mutagenesis was used to remove restriction by silent point mutations. Plasmids were isolated from transformed XL-10 Z-competent cells (Maxi Prep kit: Qiagen) and sequenced at the Leiden Genome Technology Center. Sequences were analyzed and verified (CLC Main Workbench).

Cell culture

General. HEK293T cells were kept in culture at 37 °C under 7% CO_2 in DMEM containing phenol red, stable glutamine, 10% (v/v) newborn calf serum (Thermo Fisher), and penicillin and streptomycin (200 µg/mL each; Duchefa). Medium was refreshed every 2-3 days and cells were passaged twice a week at 80-90% confluence. Cells lines were purchased from ATCC and were regularly tested for mycoplasma contamination.

Transient transfection. Transient transfection was performed as previously described.[21] In brief, HEK293T cells were seeded in 15-cm petri dishes one day prior to transfection. Prior to transfection, culture medium was aspirated and a minimal amount of medium was added. A 3:1 (m/m) mixture of polyethyleneimine (PEI, 1 mg/mL) (60 µg/15-cm dish) and plasmid DNA (20 µg/dish) was prepared in serum free culture medium and incubated for 15 min at RT. Transfection was performed by dropwise addition of the PEI/DNA mixture to the cells. Transfection with the empty pcDNA3.1 vector was used to generate control samples (mock groups). After 24 h, medium was refreshed. Medium was aspirated 72 h post-transfection and cells were harvested by resuspension in PBS. Cells were pelleted by centrifugation (5 min, 1,000 *g*) and the pellet was washed with PBS. The supernatant was discarded and the cell pellets were snap-frozen in liquid nitrogen and stored at -80 °C until sample preparation.

Sample preparation

Cell membrane and cytosol proteome preparation. Cell pellets were thawed on ice, resuspended in cold lysis buffer (50 mM Tris HCl, pH 8, 2 mM DTT, 1 mM $MgCl_2$, 2.5 U/mL benzonase) and incubated on ice (30 min). The cell lysate was collected and centrifuged (100.000 *g*, 45 min, 4 °C, Beckman Coulter, Ti 70.1 rotor). The supernatant was collected (cytosolic fraction) and the membrane pellet was resuspended in cold storage buffer (50 mM Tris HCl, pH 8, 2 mM DTT) by thorough pipetting and passage through an insulin needle (29G). Protein concentrations were determined by a Quick Start™ Bradford

Protein Assay or QubitTM protein assay (Invitrogen). Samples were flash frozen in liquid nitrogen and stored at -80 °C until further use.

Activity based protein profiling on transiently transfected HEK293T cell lysate. Gel-based activity based protein profiling (ABPP) was performed with minor alterations of the previously reported protocol.[21] For ABPP assays on HEK293T cells overexpressing PLAAT3, the cytosol proteome (0.5 mg/mL, 20 µL) was pre-incubated with vehicle (DMSO) or inhibitor (0.5 µL in DMSO, 30 min, RT) followed by an incubation with the activity based probe MB064 (final concentration: 250 nM, 20 min, RT). Final concentrations for the inhibitors are indicated in the main text and figure legends. Only cytosol proteome was used for the dose-response test in ABPP or substrate assay. Reactions were quenched with 7 µL of 4x Laemmli buffer (5 µL, 240 mM Tris (pH 6.8), 8% (w/v) SDS, 40% (v/v) glycerol, 5% (v/v) β-mercaptoethanol, 0.04% (v/v) bromophenol blue). 10 µl sample per reaction was resolved on a 10% or 15% acrylamide SDS-PAGE gel (180 V, 70 min). Gels were scanned using a ChemiDoc MP system with Cy3 and Cy5 multichannel settings (605/50 and 695/55, filters respectively) and stained with Coomassie after scanning. All experiments were performed 3 times. Fluorescence was normalized to Coomassie staining and quantified with Image Lab (Bio-Rad). IC_{50} curves were fitted with Graphpad Prism® 7 (Graphpad Software Inc.).

Computational Chemistry

Ligand preparation. Molecular structures of LEI110 and **1** were prepared for docking using Ligprep from Schrödinger.[22] Default Ligprep settings were applied: states of heteroatoms were generated using Epik at a pH 7 ± 2.[23] No tautomers were created by the program, which resulted in one standardized structure per ligand.

Protein preparation. The x-ray structure of PLAAT3 was extracted from the PDB (PDB ID: 4DOT).[7] The apo protein structure was prepared for docking with the Protein Preparation tool from the Schrödinger 2017-4 suite. Waters were removed and default protein preparation settings were applied: explicit hydrogens were added and states of heteroatoms were generated using Epik at a pH 7 ± 2, resulting in a protonated state of binding pocket His23. Additionally, missing side chains and loops were added using Prime,[24] but none were detected.

Docking. As the PLAAT3 lacked a co-crystalized ligand, induced-fit docking was applied to induce the PLAAT3 binding pocket into a ligand-binding conformation. Both LEI110 and **1** were docked with induced-fit, resulting in 39 different pocket conformations. Induced-fit docking was followed by covalent docking of LEI110 and **1** to Cys113 in all 39 generated pocket conformations. Compounds were docked using the Schrödinger 2017-4 suite[25] with SP precision. The ten poses with the lowest docking scores were manually

examined and one pose per ligand was selected. Selection was based on docking score, frequency of recurring poses, and interactions made between the ligand and the protein.

Molecular dynamics. The selected LEI110 and **1** poses in complex with PLAAT3 were simulated with molecular dynamics using Desmond Molecular Dynamics System from Schrödinger.[26] The system was setup using solvent model SPC and OPLS3 force field. The simulation was performed at a temperature of 300 Kelvin and a pressure of 1.01 bar. Triplicate runs were executed with a runtime of 100 ns per run. The simulations showed that PLAAT3 remained stable when in complex with LEI110 and **1**.

3.5 References

1. Jin, X.-H.; Uyama, T.; Wang, J.; Okamoto, Y.; Tonai, T.; Ueda, N., cDNA cloning and characterization of human and mouse Ca^{2+}-independent phosphatidylethanolamine N-acyltransferases. *BBA-Mol. Cell Biol. L.* **2009,** *1791* (1), 32-38.

2. Uyama, T.; Ikematsu, N.; Inoue, M.; Shinohara, N.; Jin, X. H.; Tsuboi, K.; Tonai, T.; Tokumura, A.; Ueda, N., Generation of N-acylphosphatidylethanolamine by members of the phospholipase A/acyltransferase (PLA/AT) family. *J. Biol. Chem.* **2012,** *287* (38), 31905-19.

3. Anantharaman, V.; Aravind, L., Evolutionary history, structural features and biochemical diversity of the NlpC/P60 superfamily of enzymes. *Genome biol.* **2003,** *4* (2), R11.

4. Kiser, P. D.; Golczak, M.; Palczewski, K., Chemistry of the retinoid (visual) cycle. *Chem. Rev.* **2014,** *114* (1), 194-232.

5. Duncan, R. E.; Sarkadi-Nagy, E.; Jaworski, K.; Ahmadian, M.; Sul, H. S., Identification and functional characterization of adipose-specific phospholipase A2 (AdPLA). *J. Biol. Chem.* **2008,** *283* (37), 25428-25436.

6. Uyama, T.; Morishita, J.; Jin, X. H.; Okamoto, Y.; Tsuboi, K.; Ueda, N., The tumor suppressor gene H-Rev107 functions as a novel Ca^{2+}-independent cytosolic phospholipase A(1/2) of the thiol hydrolase type. *J. Lipid Res.* **2009,** *50* (4), 685-693.

7. Golczak, M.; Kiser, P. D.; Sears, A. E.; Lodowski, D. T.; Blaner, W. S.; Palczewski, K., Structural basis for the acyltransferase activity of lecithin:retinol acyltransferase-like proteins. *J. Biol. Chem.* **2012,** *287* (28), 23790-807.

8. Uyama, T.; Ichi, I.; Kono, N.; Inoue, A.; Tsuboi, K.; Jin, X. H.; Araki, N.; Aoki, J.; Arai, H.; Ueda, N., Regulation of peroxisomal lipid metabolism by catalytic activity of tumor suppressor H-rev107. *J. Biol. Chem.* **2012,** *287* (4), 2706-18.

9. Akiyama, H.; Hiraki, Y.; Noda, M.; Shigeno, C.; Ito, H.; Nakamura, T., Molecular cloning and biological activity of a novel Ha-Ras suppressor gene predominantly expressed in skeletal muscle, heart, brain, and bone marrow by differential display using clonal mouse EC cells, ATDC5. *J. Biol. Chem.* **1999,** *274* (45), 32192-7.

10. Ito, H.; Akiyama, H.; Shigeno, C.; Nakamura, T., Isolation, characterization, and chromosome mapping of a human A-C1 Ha-Ras suppressor gene (HRASLS). *Cytogenet. Cell Genet.* **2001,** *93* (1-2), 36-9.

11. Uyama, T.; Inoue, M.; Okamoto, Y.; Shinohara, N.; Tai, T.; Tsuboi, K.; Inoue, T.; Tokumura, A.; Ueda, N., Involvement of phospholipase A/acyltransferase-1 in N-acylphosphatidylethanolamine generation. *Biochim. Biophys. Acta* **2013,** *1831* (12), 1690-701.

12. Shyu, R. Y.; Hsieh, Y. C.; Tsai, F. M.; Wu, C. C.; Jiang, S. Y., Cloning and functional characterization of the HRASLS2 gene. *Amino acids* **2008,** *35* (1), 129-37.

13. Uyama, T.; Jin, X.-H.; Tsuboi, K.; Tonai, T.; Ueda, N., Characterization of the human tumor suppressors TIG3 and HRASLS2 as phospholipid-metabolizing enzymes. *BBA-Mol. Cell Biol. L.* **2009,** *1791* (12), 1114-1124.

14. Jaworski, K.; Ahmadian, M.; Duncan, R. E.; Sarkadi-Nagy, E.; Varady, K. A.; Hellerstein, M. K.; Lee, H.-Y.; Samuel, V. T.; Shulman, G. I.; Kim, K.-H.; de Val, S.; Kang, C.; Sul, H. S., AdPLA ablation increases lipolysis and prevents obesity induced by high-fat feeding or leptin deficiency. *Nat. Med.* **2009,** *15*, 159.

15. DiSepio, D.; Ghosn, C.; Eckert, R. L.; Deucher, A.; Robinson, N.; Duvic, M.; Chandraratna, R. A. S.; Nagpal, S., Identification and characterization of a retinoid-induced class II tumor suppressor growth regulatory gene. *Proc. Natl. Acad. Sci. U. S. A.* **1998,** *95* (25), 14811-14815.

16. Wu, C. C.; Shyu, R. Y.; Wang, C. H.; Tsai, T. C.; Wang, L. K.; Chen, M. L.; Jiang, S. Y.; Tsai, F. M., Involvement of the prostaglandin D2 signal pathway in retinoid-inducible gene 1 (RIG1)-mediated suppression of cell invasion in testis cancer cells. *Biochim. Biophys. Acta* **2012,** *1823* (12), 2227-36.

17. Duvic, M.; Helekar, B.; Schulz, C.; Cho, M.; DiSepio, D.; Hager, C.; DiMao, D.; Hazarika, P.; Jackson, B.; Breuer-McHam, J.; Young, J.; Clayman, G.; Lippman, S. M.; Chandraratna, R. A.; Robinson, N. A.; Deucher, A.; Eckert, R. L.; Nagpal, S., Expression of a retinoid-inducible tumor suppressor, Tazarotene-inducible gene-3, is decreased in psoriasis and skin cancer. *Clin. Cancer Res.* **2000,** *6* (8), 3249-59.

18. Yamano, Y.; Asano, A.; Ohyama, K.; Ohta, M.; Nishio, R.; Morishima, I., Expression of the Ha-ras suppressor family member 5 gene in the maturing rat testis. *Biosci. Biotech. Bioch.* **2008,** *72* (5), 1360-3.

19. Jin, X. H.; Okamoto, Y.; Morishita, J.; Tsuboi, K.; Tonai, T.; Ueda, N., Discovery and characterization of a Ca^{2+}-independent phosphatidylethanolamine N-acyltransferase generating the anandamide precursor and its congeners. *J. Biol. Chem.* **2007,** *282* (6), 3614-23.

20. De Risi, C.; Pollini, G. P.; Zanirato, V., Recent developments in general methodologies for the synthesis of α-ketoamides. *Chem. Rev.* **2016,** *116* (5), 3241-3305.

21. Baggelaar, M. P.; Janssen, F. J.; van Esbroeck, A. C. M.; den Dulk, H.; Allara, M.; Hoogendoorn, S.; McGuire, R.; Florea, B. I.; Meeuwenoord, N.; van den Elst, H.; van der Marel, G. A.; Brouwer, J.; Di Marzo, V.; Overkleeft, H. S.; van der Stelt, M., Development of an activity-based probe and in silico design reveal highly selective inhibitors for diacylglycerol lipase-alpha in brain. *Angew. Chem.-Int. Edit.* **2013,** *52* (46), 12081-12085.

22. Schrödinger. Release 2017-4, LigPrep, Schrödinger, LLC, New York, NY, **2017**.

23. Schrödinger. Release 2017-4, Epik, Schrödinger, LLC, New York, NY, **2017**.

24. Schrödinger. Release 2017-4: Prime, Schrödinger, LLC, New York, NY, **2017**.

25. Schrödinger. Small-Molecule Drug Discovery Suite 2017-4, Schrödinger, LLC, New York, NY, **2017**.

26. Schrödinger. Release 2017-4: Desmond Molecular Dynamics System, D. E. Shaw Research, New York, NY, **2017**. Maestro-Desmond Interoperability Tools, Schrödinger, New York, NY, 2017.